INVESTIGATION ON CENTRIFUGAL PUMP PERFORMANCE DEGRADATION UNDER AIR-WATER INLET TWO-PHASE FLOW CONDITIONS

Qiaorui SI [(1)], Qianglei CUI[(3)], Keyu ZHANG[(2)], Jianping YUAN[(4)], Gérard BOIS[(5)*]

[(1)] National Research Center of Pumps, Jiangsu University, Zhenjiang, China, 212013, e-mail: siqiaorui@163.com
[(2)] National Research Center of Pumps, Jiangsu University, Zhenjiang, China, 212013, e-mail: zhangky189@163.com
[(3)] National Research Center of Pumps, Jiangsu University, Zhenjiang, China, 212013, e-mail: 786485282@qq.com
[(4)] National Research Center of Pumps, Jiangsu University, Zhenjiang, China, 212013, e-mail: yh@ujs.edu.cn
[(5)] LML, UMR CNRS 8107, Arts et Métiers ParisTech, Lille, France, 59000, e-mail: gerard.bois@ensam.eu

In order to study the flow characteristics of centrifugal pumps when transporting the gas-liquid mixture, water and air were chosen as the working medium. Both numerical simulation and experimental tests were conducted on a centrifugal pump under different conditions of inlet air volume fraction (IAVF). The calculation used URANS k-epsilon turbulence model combined with the Euler-Euler inhomogeneous two-phase model. The air distribution and velocity streamline inside the impeller were obtained to discuss the flow characteristics of the pump. The results shows that air concentration is high at the inlet pressure side of the blade, where the vortex will exist, indicating that the gas concentration have a great relationship with the vortex aggregation in the impeller passages. In the experimental works, pump performance were measured at different IAVF and compared with numerical results. Contributions to the centrifugal pump performance degradations were analyzed under different air-water inlet flow condition such as IAVF, bubble size, inlet pressure. Results show that pump performance degradation is more pronounced for low flow rates compared to high flow rates. Finally, pressure pulsation and vibration experiments of the pump model under different IAVF were also conducted. Inlet and outlet transient pressure signals under four IAVF were investigated and pressure pulsation frequency of the monitors is near the blade passing frequency at different IAVF, and when IAVF increased, the lower frequency signal are more and more obvious. Vibration signals at five measuring points were also obtained under different IAVF for various flow rates.

Key words:

Pump Performance, Two-Phase flow, Numerical-Experiment Comparisons, Vibration

Analyse de la dégradation des performances de pompes centrifuges en présence de mélange diphasique air-eau en entrée de roue

Un mélange diphasique air-eau alimente une pompe centrifuge pour en étudier les modifications de performance par rapport à de l'eau pure. Les analyses sont conduites à l'aide de simulations numériques et des expériences pour différentes valeurs de fraction volumique du mélange en entrée de la pompe. La simulation numérique utilise une approche instationnaire URANS avec le modèle de fermeture turbulente k-epsilon associé à une description Eulérienne pour chaque fluide, l'ensemble étant traité comme un milieu inhomogène. La distribution locale des caractéristiques du mélange ainsi que des lignes de courant à l'intérieur de la pompe et plus particulièrement de la roue sont utilisés pour permettre une analyse locale détaillée en particulier de l'évolution de la fraction volumique. La concentration d'air est importante à l'entrée de la roue et sur la face en pression des aubages dans les zones de forts gradients et les zones où se concentrent les zones tourbillonnaires à l'intérieur des passages inter-aubes. Les analyses portent prennent également en compte, outre différentes valeurs de la fraction volumique initiale, les variations du diamètre des bulles d'air et celles du débit global traversant la pompe. Les modifications des performances globales de la pompe, mesurées expérimentalement, sont plus importantes vers les bas débits. Elles sont confirmées, qualitativement et quantitativement par l'approche numérique retenue. Les mesures complémentaires de fluctuations de pressions en entrée et en sortie de pompe ainsi que des mesures de vibration sur le corps de pompe permettent une analyse en fréquence des signaux et leur mise en relation avec les résultats numériques sur les caractéristiques locales des écoulements

Mots-clefs :

Pompe, Ecoulement diphasique, Comparaisons calculs-expériences, vibrations.

I INTRODUCTION

Two-phase gas-liquid flows often happened in air conditioning systems, refrigerating, cryogenic, petroleum, nuclear power and also in sewage treatment. Centrifugal pumps play important roles in all these fields. It is well known that pump head will decrease under two-phase mixture conditions

compared to single-phase one. The degree of head degradation depends on geometrical, physical and thermal conditions (Gülich [2014]). For a given pump geometry and increasing value of void gas fraction, the head can be totally lost, the consequence of which can result in huge system instabilities and pump degradations.

Several authors like Murakami et al. [1974a], Minemura et al. [1985] have proposed prediction methods for the two-phase flow performances on axial and centrifugal type of pumps in order to evaluate existing experimental measurement results with some visualization technique as well. A non-exhaustive list of important published works is proposed in Si et al. paper [2017]. All these models can be considered to be valid for low values of volumetric void fraction (max. 6%-7%) and so, far from surge operating conditions that correspond to a rapid performance decrease of the pump, the rate of which depend on the initial water flow rate. Just before such severe conditions, several investigations have detected the presence of stationary bubbles at impeller entrance channels for high gas fractions, being responsible for performance degradation of the pump (Murakami and Minemura [1974 b]; Patel and Rundstadler[1978]; Sekoguchi [1984]. Estevam[2003] and Barrios and Prado [2009]. Numerical simulations using URANS approach have been also performed in order to determine local phenomena more precisely in such flow conditions. All numerical results have in common that they show significant deviations between predicted and experimental overall results for the head drop especially for gas fraction values higher than 6%. Recently, Müller at al. [2015], have performed numerical calculation using a mono dispersed phase distribution model, the results of which are compared with experimental results obtained from Kosyna[2001]. The comparison on impeller blade static pressure distributions showed that some improvement should be done for high flow rate in order to get better fit between numerical and experimental results. However, most of the centrifugal pump impeller geometries that have been studied are designed using two dimensional blade sections and constant passage width along the radius from leading to trailing edge. There is still a need of experimental results combined with numerical ones to explain the dynamic characteristics of centrifugal pump under air-water two-phase flow working condition.

In the present paper, experimental and numerical comparisons results are presented on two- phase flow performance in a centrifugal pump designed with three dimensional shrouded impeller shape. Numerical results have been performed using inhomogeneous model (instead of usually homogeneous model), for which each fluid possesses its own flow field and the fluids interact via interphase transfer terms and compared with overall experimental ones. In addition, inlet and outlet transient pressure and vibration signals under four IAVF are analyzed with frequency to investigate the dynamic characteristics.

II PUMP GEOMETRY AND TEST RIG ARRANGEMEMENT

A commercial single stage, single-suction, horizontal-orientated centrifugal pump with specific speed (Ωs= 65) was used for the investigation, whose casing is typically combined with a spiral-volute. The design parameters and global pump geometry, given by the manufacturer, can be found in Si et al. [2017]. The test rig is schematically shown on Figure 1. In this open loop, air injection system is driven by a compressor. Air flowrate is measured by micro-electro mechanical systems flow sensors, which could supply volume air flowrate value on standard conditions (25°, 101325Pa). Air-water flow is sucked by the pump, goes through the regulating valve and finally arrives into the downstream tank. Air bubbles exhaust to external space in open tank and the left pure water run to the upstream tank. Volume flowrate of pure water was measured by an electromagnetic flowmeter set between upstream tank and the air supply device. Pump head and global efficiency is also obtained following ISO 9906: 2012.

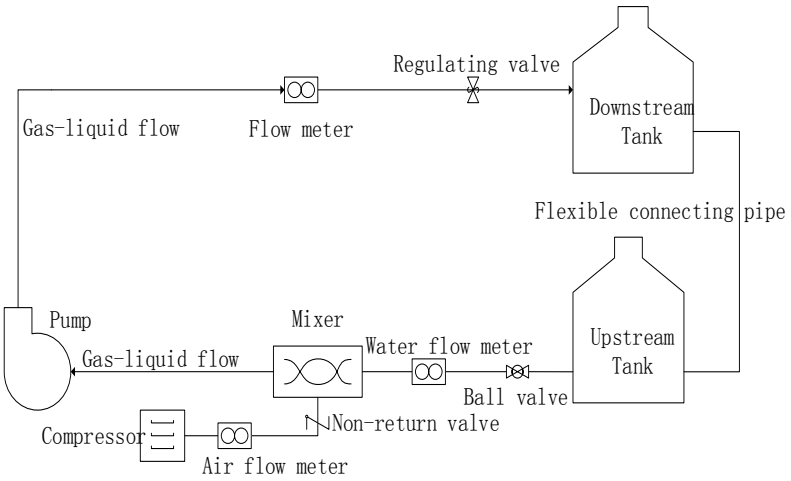

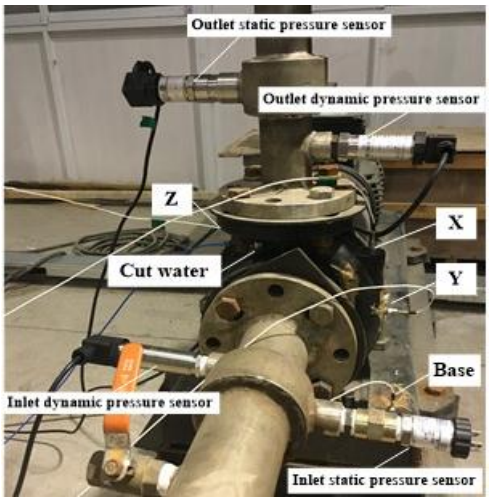

Figure 1: *Test rig* **Figure 2:** *Sensor locations*

It has to be noticed that the inlet pipe loop is in horizontal and part of the inlet tubing is transparent in order to observe the inlet bubble distribution. This allows see a rough global view of bubbles size. At this step, only air volume flow rate is measured, bubble diameter distribution including bubble number per volume at pump inlet is not available. Measurements are performed using the followed procedures: a constant void fraction is set by changing the throttle vane position and consequently obtained the corresponding water flow rate. Inlet air volume flow rate was transferred after knowing the pump inlet pressure value from the inlet static pressure sensor in order to calculate the inlet air void fraction. Measurement uncertainties calculated by instrument precision are 0.33m error on pump head and 2.4% on pump global efficiency. Figure 2 shows a general view of sensor locations close to the pump environment.

III EXPERIMENTAL PUMP PERFORMANCE CHARACTERISTICS

The test loop condition were that 2m water high level inside the tank, air injection is performed with the same inlet compressor pressure mainly 60kPa. Four injecting tubes around the inlet pipe section inject air bubbles with the same direction of the water flow. The above loop setting could ensure that no cavitation happened during the experiment process. The water flow rate is kept constant, changing the air injecting flow rate and get inlet air void fraction values at 1%, 3%, 5%, 8%, 9% and 10%.

Figure 3a shows pump performance curves at different given void fraction values. It can be seen, as already pointed out by several previous researchers, that pump performance starts to be significantly lower when void fraction reaches 3% and more. The value of the head performance degradation also depends on the water flow rate. A decrease of 20% of head compared with single phase shut-off conditions is achieved for all water flow rates below nominal conditions for void fraction going up to 7%. Lowest void fraction up to 10% can be achieved without pump surge for water flow rates around 32~40 m^3/h. These values correspond to 0.7 up to 0.8 Q_d, compared to a manufacturer given operating pump flow rate of 50.6m^3/h. Other two phase flow experimental results are also plotted in Figure 3b, using the theoretical head coefficient. All points are on a quite unique curve whatever the void fraction value is. This result validates all semi-empirical and one dimensional model assumptions that have been used for most existing approaches in the literature for such a pump geometry. As a consequence, efficiency values (from Si et al [2017]) are always lower than efficiency for zero void fraction, which is obviously normal due to increasing impeller passage losses when two-phase flow conditions are existing. One can also observed that maximum efficiency locations are displaced towards lower water flow rates when void fraction is increasing. This can be attributed to blockage effects at impeller inlet section which may modify the incidence angle values.

IV NUMERICAL SIMULATION ANALYSIS

With the validated CFD model, values of blade forces, pressure heads, and inlet air void fraction (IAVF) distributions inside the pump can be analysed. These values are very difficult and expensive to be measured using experimental instrumentation. All of this could help us well understand inner flow characteristics of centrifugal pump working under air-water two-phase flow condition.

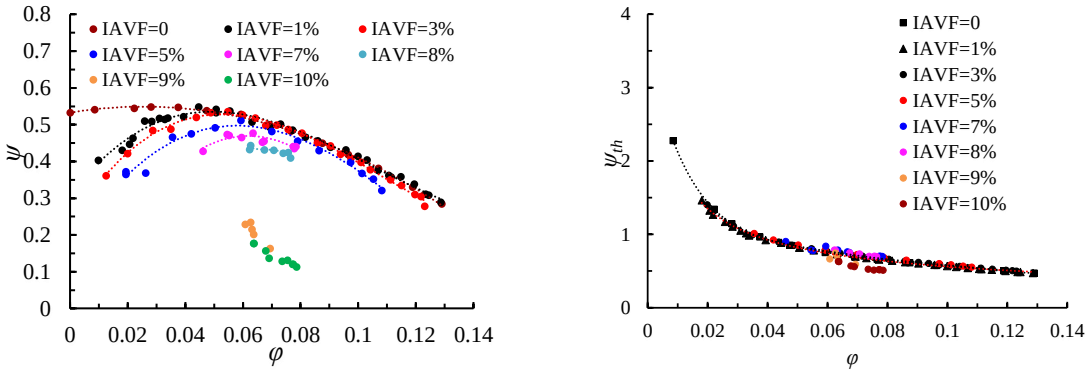

(a) Head coefficient (b) Theoretical head coefficient

Figure 3: *Pump performance modification for different values of IAVF*

IV.1 PUMP MODEL AND MESHES

The pump was divided into five component parts such as the inlet, impeller ring, chamber, impeller and volute to build a model mesh for a complete pump. This process would allow each mesh to be individually generated and tailored to the flow requirements in that particular component. The influence of boundary conditions was investigated to discard any effect on the numerical results, particularly on the inlet and outlet part. These last two parts are extended to assure that the flow closed to inlet and outlet parts corresponds to a fully developed condition.The grids for the computational domains were generated using ANSYS ICEM-CFD14.5 with blocking method. The independence of the solutions from the number of grid elements was proven by simulating the flow field with different numbers of grid elements, as shown in Figure 4a. The resulting pump model consisted of 2775915 elements was chosen for rotating and stationary domains in total. Structured hexahedral cells were used to define the calculation domains, whose detail are shown in Figure 4b.

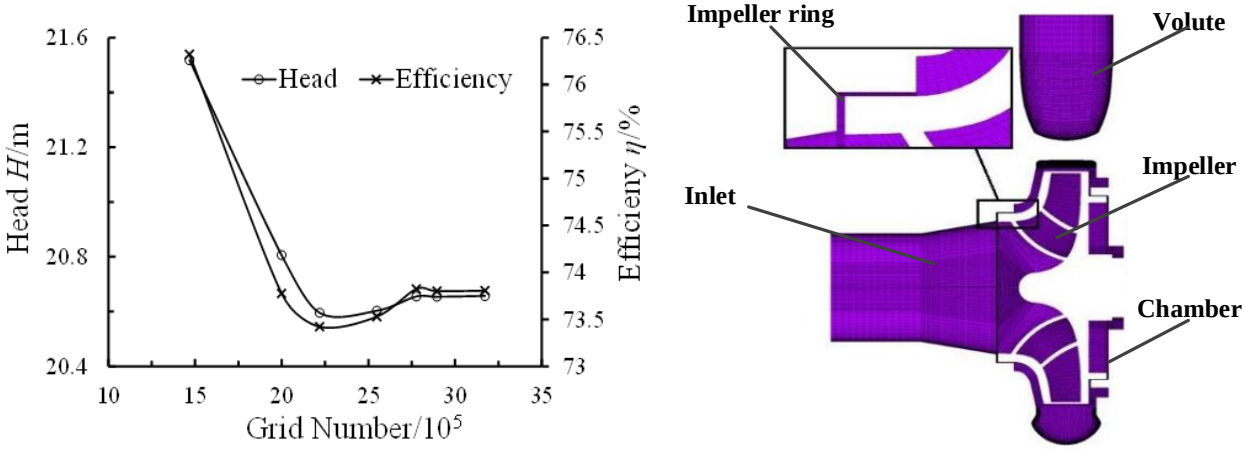

(a) Grid number dependence (b) Structure Mesh

Figure 4: *Three dimensional numerical domain with local meshing*

IV.2 BOUNDARY CONDITION AND NUMERICAL MODELS

The professional CFD software ANSYS CFX14.5 was used for the simulation. Three dimensional URANS equations were solved using the *k-e* turbulence model, with boundary conditions of total pressure at the inlet and mixture mass flow rate at the outlet. Smooth wall

condition was used for the near-wall function. Inhomogeneous model also named the inter-fluid transfer model was chosen to adapt the Eulerian-Eulerian multiphase flow. In this model each fluid possesses its own flow field and the fluids interact via interphase transfer terms. Thus, this model provides one solution field for each of the separate phases. Transported quantities interact via interphase transfer terms. Furthermore, particle model is applied for the interphase transfer terms, which is suitable for modeling dispersed multiphase flow problems such as the dispersion of air bubbles in a liquid. Initial bubble diameter set as 0.1mm and 0.2mm.

The interface between the impeller and the casing is set to "transient rotor-stator" to capture the transient rotor-stator interaction in the flow, because the relative position between the impeller and the casing was changed for each time step with this kind of interface. The chosen time step (Δt) for the transient simulation is 1.718×10^{-4} s for nominal rotating speed, which corresponds to a changed angle of 3°. Within each time step, 20 iterations were chosen and the iteration stops when the maximum residual is less than 10^{-4}. Ten impeller revolutions were conducted for each operational condition in order to reach stable periodicity results for convergence criteria, and the last four revolutions results were kept for analysis.

It is quite well known that unsteady calculation is mandatory for rotating machinery analysis when looking at rotor-stator interaction problems instead of steady conditions. This is more evident when two-phase flows are investigated. As an example, figure 5 illustrates the big differences on air void fraction distribution inside the impeller corresponding for both two approaches.

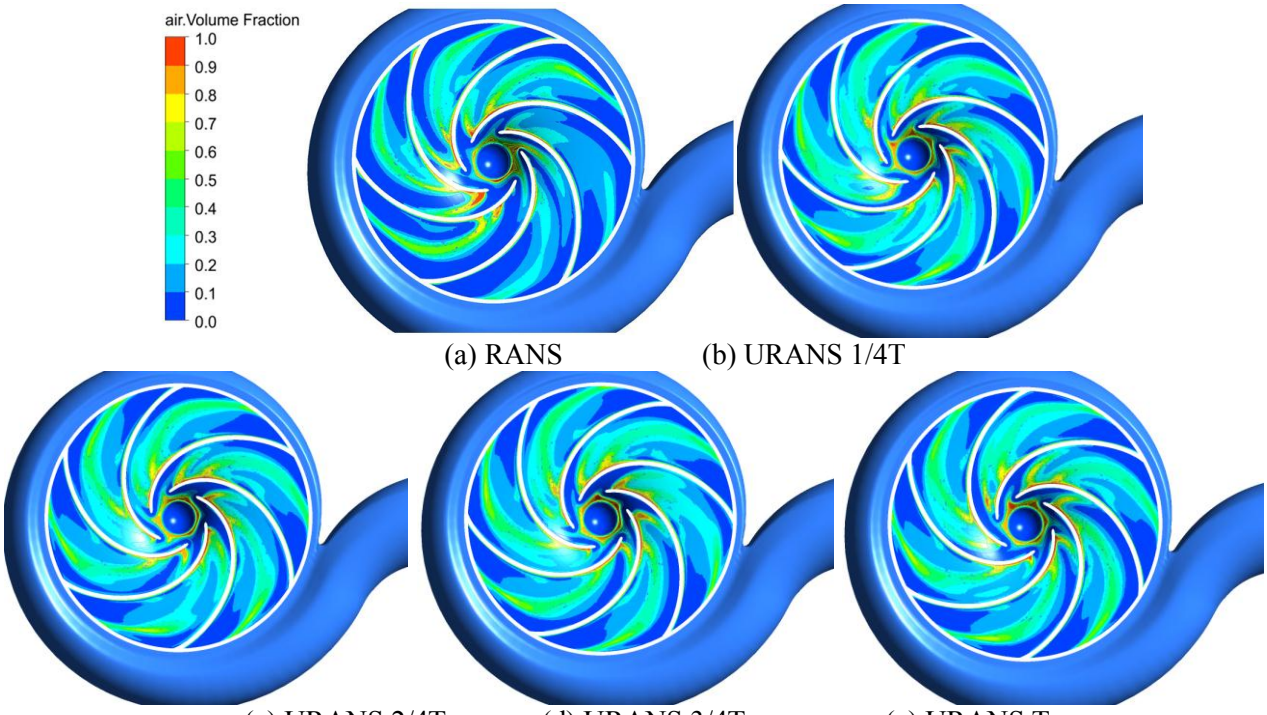

(a) RANS (b) URANS 1/4T

(c) URANS 2/4T (d) URANS 3/4T (e) URANS T

Figure 5: *Example of void fraction distribution inside the impeller passage*

IV.3 Numerical results

IV.3.1 Pump performance comparison between the simulation and experiment

Comparisons between simulation and experiment when pump works at pure water condition are quite good as already shown in a previous publication done by the same research team (SI et al. [2017]). This means that the calculated domain, meshes, boundary condition and numerical turbulence models are suitable for further analysis. Performance curves of numerical simulation and experiment with different IAVF are shown in Figure 6. Numerical results show that the calculation is quite sensitive to initial bubble diameter value for small flow rates. Numerical results are quite comparable up IAVF= 7% for the adapted bubble diameter. From experimental investigation, it seems that pump performance is less sensitive to inlet bubble diameter values than numerical results.

198 This result also needs more investigation in order to explain it. The simulation results are believable
199 if the adequate initial bubble diameter is chosen.

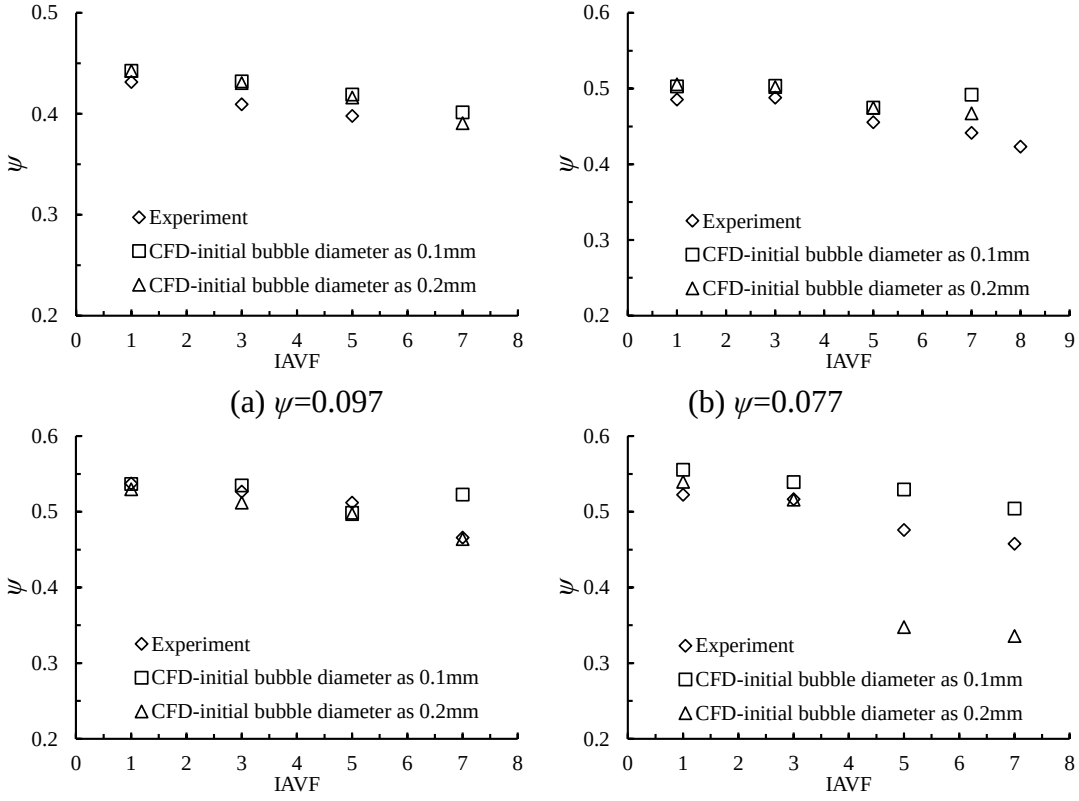

200

201 (a) ψ=0.097 (b) ψ=0.077

202

203 (c) ψ=0.059 (d) ψ=0.039

204 **Figure 6:** *Comparisons of head pump coefficient for different IAVF values*

205 **Table 1:** *Air distribution in middle section of the pump under different IAVF*

Flow rate	Scale	IAVF=1%	IAVF=5%	IAVF=7%
0.6 Q_d	1.0 0.9 0.8 0.7 0.6 0.5 0.4 0.3 0.2 0.1 0.0		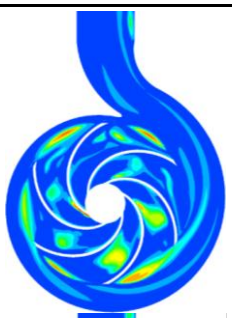	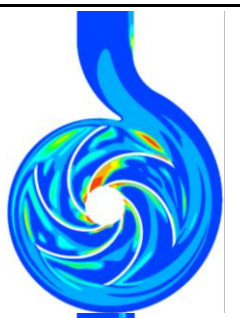
0.8 Q_d			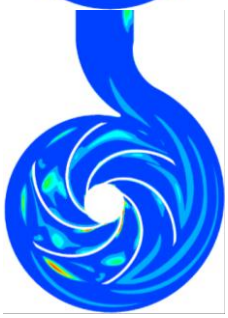	

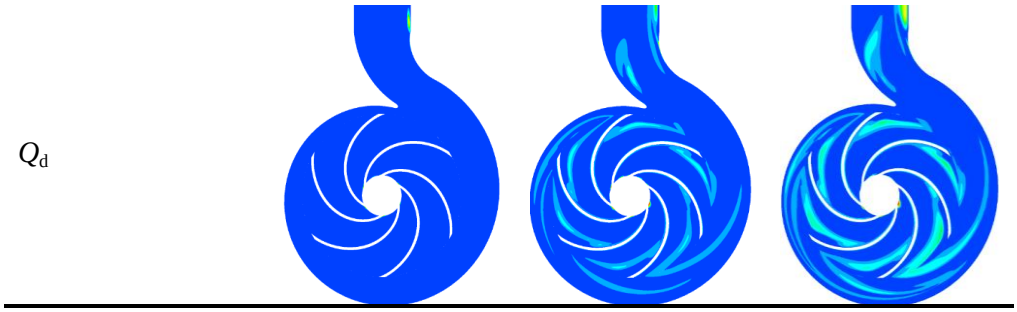

IV.3.2 Flow analysis inside the impeller and volute

The transport air-water ability of the pump mainly depends on air and water distributions inside the flow channel. Table 1 shows the local air void fraction distribution inside the impeller and volute channel for three flow rate and for three IAVF values. It can be seen that air void fraction is bigger inside the impeller than volute channel for all three flow rates and all three IAVF. Air bubbles distribute on pressure side of the blade and are detained more and more inside the impeller channel near "wake" area when IAVF increase. Bubbles take over 60% part of the channel when IAVF increase to 7% in all three flowrates, which is probably the reason why pump performance breaks down. The biggest value of air void fraction decrease as pump flowrate increase, which means centrifugal pump are more sensitive to the air at small flow rates. Air bubbles are also detected on blade pressure side from leading edge to the middle channel parts. Further investigations from numerical results are needed in order to evaluate high loss locations due two phase conditions and on impeller blade static pressure distribution as pointed out in the conclusions of Müller's paper [2015].

IV.3.3 Unsteady pressure evolution

Numerical unsteady pressure evolution results, corresponding to position p1-p6, are given on figure 7a. Temporal pressure coefficient evolution results are obtained for a flow rate equivalent to Q/Q_d=0.8, as is shown in figure7b. The corresponding FFT chart is given on figure 7c. Comparative FFT chart under $0.6Q_d$ is given on figure 7d. One can detect that pressure fluctuations are stronger when inlet void fraction increases with a maximum power value for 5% at blade passing frequency value. Amplitude of the pressure cofficient always present bigger values if the monitoring points near the volute tongue. FFT results of the pressure cofficient at the two flowrates show the same variation law when IVAF increase. Smaller flowrate give more low frequency characteristic.

When looking at vibration results (which are presented in the next section), same kind of results can be found. It is interesting to notice, as already pointed out in section IV.3.2 that this corresponds to the fact that regions with high void fraction levels are not any more close to the impeller walls but are pushed in the main flow when flow rate is decreasing and IAVF is close to 5% (see results also from Table 1) .

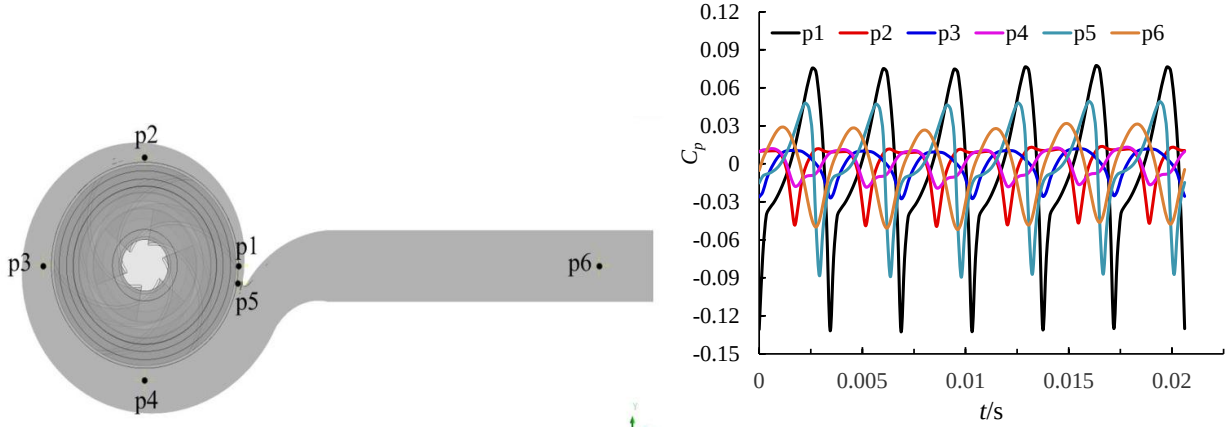

(a) Location of monitoring points (b) Temporal pressure coefficient evolution when IAVF=3%

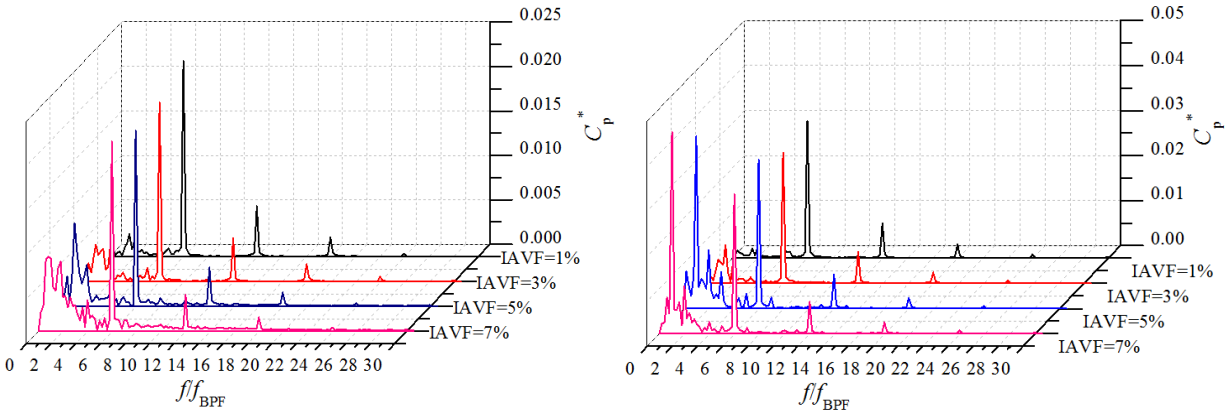

(c) FFT results at p6 when $0.8Q_d$ (d) FFT results at p6 when $0.6Q_d$

Figure 7: *Unsteady pressure evolution of the monitoring points*

IV.3.4 Casing vibration experimental results

Part of vibration results, obtained by accelerometer X (radial position- see figure 2), are given using FFT analysis for the same flow rate Q/Q_d=0.8 and for several IAVF conditions. It can be seen, from figures 8a to 8e, that maximum acceleration amplitude always occur at blade passing frequency (6 impeller blades). When IAVF increases, lower frequencies appear with growing amplitude corresponding to one and three blades. The average value of acceleration severity (all frequencies are taken into account) is given in figure 8f. It can be observed that maximum severity levels are obtained for IAVF values close to 5-6% and then tend to decrease. It is believed that unsteady experimental results agree, at least qualitatively, with what have been obtained with the chosen numerical approach. This has also been experimentaly pointed out in the conclusion of Kosyna's paper [2001] using unsteady measurements performed on the rotating impeller close to outlet radius. More deep analysis is in progress in order to extract more detailed informations in particular for lower flow rates.

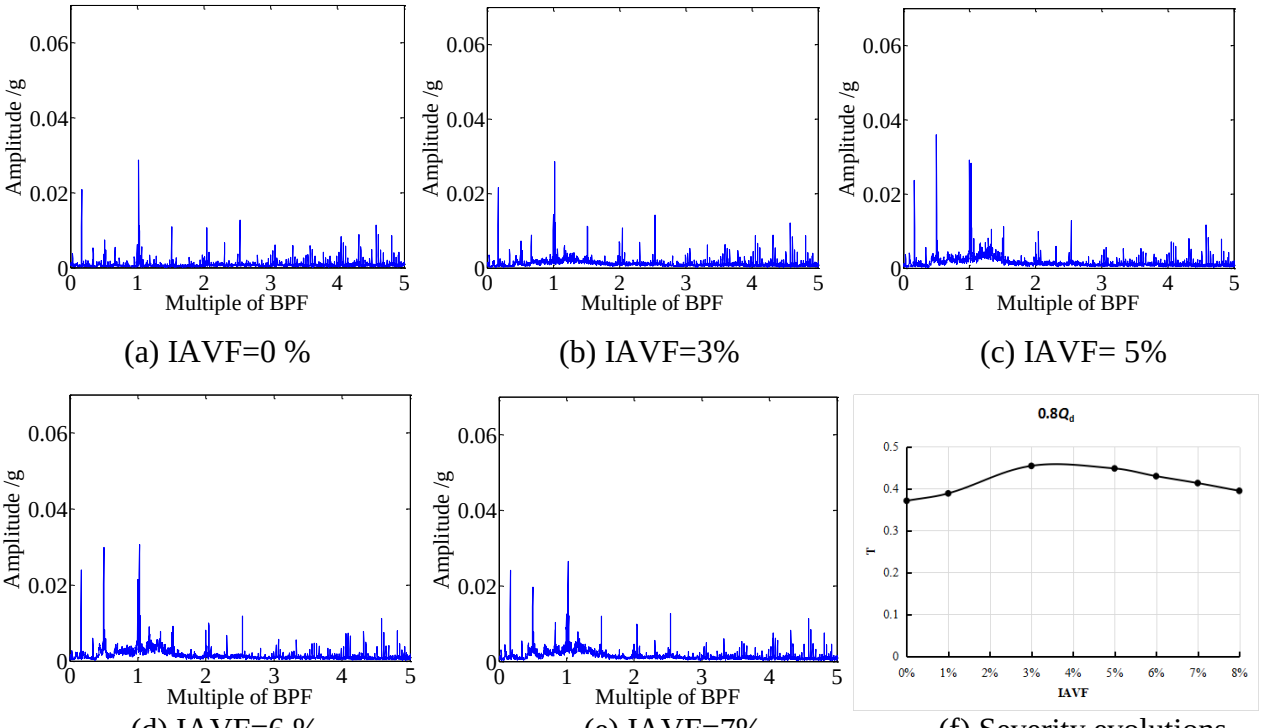

(a) IAVF=0 % (b) IAVF=3% (c) IAVF= 5%

(d) IAVF=6 % (e) IAVF=7% (f) Severity evolutions

Figure 8: *FFT acceleration levels (X direction) for several IAVF values at Q/Q_d=0.8*

V CONCLUSIONS

Experimental overall pump performances and dynamic characteristics have been performed under air-water two phase conditions for a centrifugal geometry. Local flow pattern inside the pump have been also obtained using CFD tools in order to explain the performance degradation when IAVF was increased. The main results are the following:

1. Pump performance degradation is more pronounced for low flow rates compared to high flow rates. The starting point of severe pump degradation rate is related a specific flow coefficient, which value corresponds to the change of the slope of the theoretical head curve.
2. Compared with existing experimental results for 2D impeller shapes, the present 3D impeller pump geometry head degradation is quite small (less than 1%) within IAVF values below 5% between $0.75Q_n$ and Q_n.
3. Local numerical results inside the impeller and volute passages give some explanation about this last point and describe the air-water flow pattern change just before the experimental pump breakdown. Particle fluid model with interface transfer terms looks quite suitable to evaluate pump performance degradation up to IAVF values of 7%.
4. Maximum experimental IAVF of 10% can be reached before pump breakdown only for initial inlet flow conditions close to best efficiency ones. Numerical approach always fails using high IAVF inlet conditions.
5. Pressure fluctuations are stronger when inlet void fraction increases with a maximum power value for 5% at blade passing frequency value and small flowrate would be given more low frequency characteristics. Maximum severity levels of vibration are obtained for IAVF values close to 5-6% and then tend to decrease.

VI NOMENCLATURE

b: impeller blade width
u: circular velocity
R: radius
n: rotational speed
p: static pressure
C_p: local pressure coefficient $C_p = \dfrac{p - \bar{p}}{0.5\rho u_2^2}$
H: pump head
Q: volume water flow rate
t: time
α: local air void fraction
φ: flow coefficient $\varphi = Q/(2\pi \cdot R_2 \cdot b_2 \cdot u_2)$
ρ: density of mixed fluid $\rho = \rho_{water} \times (1-\alpha) + \rho_{air} \times \alpha$
v: water cinematic viscosity
ω: angular velocity
η: global efficiency of the pump $\eta = \dfrac{\rho g Q_{water} H}{P}$
ψ: head coefficient $\psi = gH/(u_2)^2$
ψ_t: theoretical head coefficient $\psi_{t=} \psi/\eta$
Ωs*:* specific speed $\Omega s = \omega \cdot \dfrac{Q^{0.5}}{(gH)^{0.75}}$
Z: impeller blade number
BPF: blade passing frequency
d: design condition
IAVF: Inlet air void fraction $IAVF = \dfrac{Q_{air}}{Q_{air} + Q_{water}}$

T: vibration severity $T = \sqrt{\frac{1}{N}\sum_{k=1}^{N} X_k^2}$

*: result from FFT

VII ACKNOWLEDGEMENTS

The authors gratefully acknowledge the financial support by National Natural Science Foundation of China (51509108), Natural Science Foundation of Jiangsu Province (BK20150516), China Postdoctoral Science Foundation Funded Project (2015M581735, 2016T90422) and Senior Talent Foundation of Jiangsu University (15JDG048).

VIII REFERENCES

Barrios, L., Prado, M. G. (2009). Modeling Two Phase Flow Inside an Electrical Submersible Pump Stage. ASME 2009, International Conference on Ocean, Offshore and Arctic Engineering (Vol.133, pp.227-231).

Estevam, V., França, F.A., Alhanati, F.J.S., (2003), Mapping the Performance of Centrifugal Pumps under Two- Phase Conditions, 17th International Congress of Mechanical Engineering, SaoPaulo.

Gülich, I. J. F. (2014). Design of the Hydraulic Components. Centrifugal Pumps. Springer Berlin Heidelberg.

Kosyna, G., Suryawijaya,P., Froedrichs,J., (2001), Improved Understanding of Two-Phase Flow Phenomena Based on Unsteady Blade Pressure Measurements, Journal of Computational and Applied Mechanics, Vol. 2, N1, pp. 45-52.

Minemura, K., Murakami,M., Katagiri,H., (1985). Characteristics of Centrifugal Pumps Handling Air-Water Mixtures and Size of Air Bubbles in Pump Impellers, Bulletin of JSME, Vol. 28, N244, pp 2310- 2318.

Müller, T., (2015).Numerical 3D RANS Simulation of Gas-Liquid Flow in a Centrifugal Pump with an Euler-Euler Two-Phase Model and a Dispersed Phase Distribution, 11thEuropean Conference on Turbomachinery Fluid dynamics & Thermodynamics, ETC11, March 23-27, ETC2015-076, Madrid.

Murakami, M., Minemura, K., (1974a). Effects of Entrained Air on the Performance of a Centrifugal Pump. Fisrt report- Performance and Flow Conditions, Bulletin of JSME, Vol. 17, N.110, pp 1047-1055.

Murakami, M., Minemura, K., (1974b). Effects of Entrained Air on the Performance of a Centrifugal Pump. Second Report- Effect of Number of Blades, Bulletin of JSME, Vol.17, N.112, pp 1286-1295.

Patel,B.R., Rundstadler, P.W., (1978). Investigation into the Two-Phase Behaviour of Centrifugal Pumps, ASME Symposium on Polyphase Flow in Turbomachinery- San Francisco-USA.

Sekoguchi, K., Takada, S., Kanemori, Y. (1984). Study of Air-Water Two-Phase Centrifugal Pump by Means of Electric Resistivity Probe Technique for Void Fraction Measurement: 1st Report, Measurement of Void Fraction Distribution in a Radial Flow Impeller. Bulletin of JSME, Vol.27, N.227, pp 931-938.

Si, Q., Bois' G., Zhang' K., Yuan' S., (2017). Air-Water Two-Phase Flow Experimental and Numerical Analysis in a Centrifugal Pump. Proceedings of 12th European Conference on Turbomachinery Fluid Dynamics and Thermodynamics, ETC 12, Stockholm, April 3-7th